

ISWI and associated activities in Slovakia: 2018

Ivan Dorotovič, Slovak Central Observatory,
Hurbanovo; ivan.dorotovic@suh.sk

*Based on individual activities of the Institutes
of the Slovak Academy of Sciences, the Universities,
Astronomical Observatories and the SCO
in Hurbanovo*



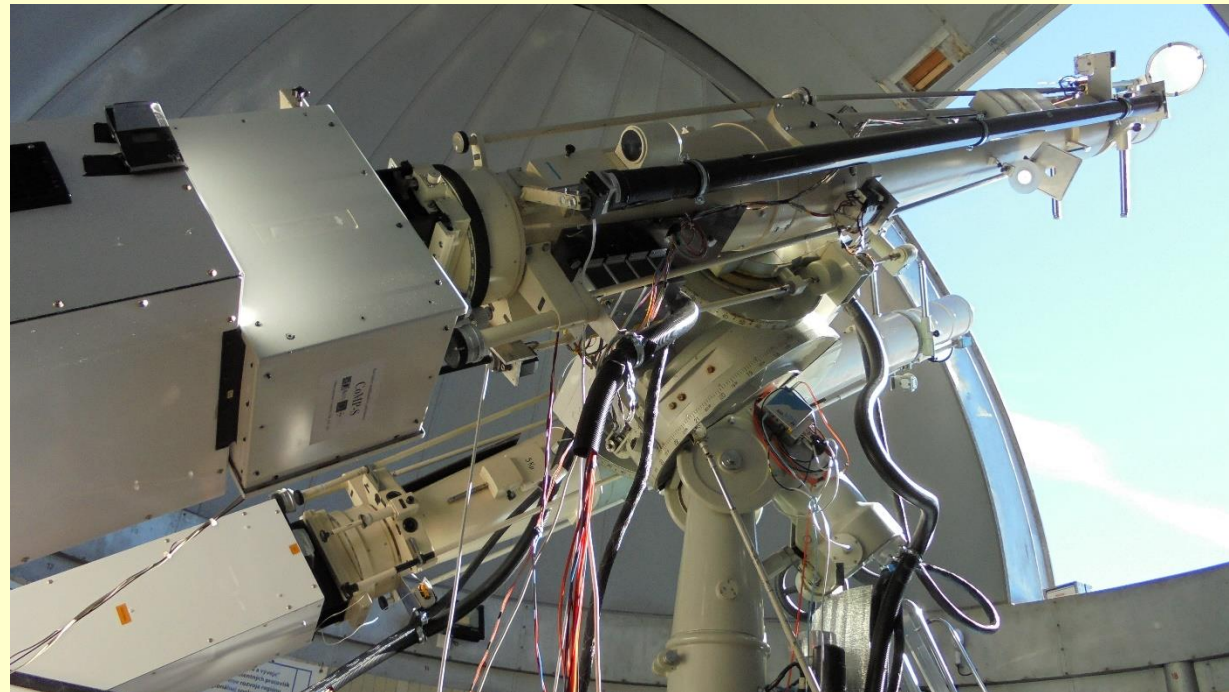
ISWI Slovakia website:

http://stara.suh.sk/id/iswi/iswi_SK-en.htm

- **Astronomical Institute of SAS, Tatranská Lomnica**

- Lomnický Peak Observatory - the COMP-S and SCD instruments:**

- the post-focus instruments for spectropolarimetry of the solar corona, prominences, active regions and filaments in the testing phase
- both based on the Lyot filter with the polarimeter for the VIS and near IR wavelength ranges (500-1100nm)
- the first observing programs: total mass of the quiet prominences, prominence legs and possible tornadoes, emergence of active regions and filaments



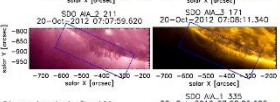
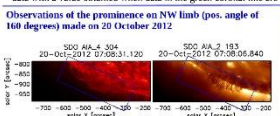
<https://www.astro.sk/l3.php?p3=lso>

The very first results presented already at the ESPM-15 in September 2017 in Budapest and the new ones will be delivered at the 2nd China-Europe Solar Physics Meeting at Hvar in May 1019

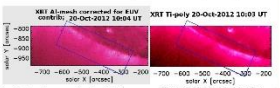
Total mass of prominences estimated from their observations in EUV, X-rays, H α and the green coronal line

P. Schwartz, J. Rybák, P. Heinzel, A. G. Tlatov, S. A. Guseva, P. Gómský, J. A. Kučera
 Astronomical Institute, Slovak Academy of Sciences of the Czech Republic, *Kislovodsk Mountain Astronomical Station of the Pulkovo observatory

ABSTRACT
 Several prominences were observed during a coordinated campaign in October 2012 in the H α and Ca II 854.2 nm lines by the COMPS instrument at the Lomnický Peck Observatory (AAS, Slovakia). Full-disk observations in soft X-rays made by the XRT instrument on-board of the Hinode satellite were also obtained during the campaign. Co-temporal coronagraphic observations in the green coronal line around the whole disk obtained at the Kislovodsk observatory and full-disk EUV images made by AIA instrument on-board of the SDO satellite were also used. The optical thickness, τ_{500} , of the microtubule and subsequently column mass of the prominence plasma composed mainly from hydrogen and helium were derived from the EUV and X-ray data using the same method as in Schwartz et al. (2016). The method is based on two mechanisms which cause intensity decrease at a prominence – the absorption in H α and He resonance continua and coronal emissivity deficit in the volume occupied by cool prominence plasma. Total mass of a prominence can be then calculated as an integration of the column mass over the area of a prominence. In this work we compare value of total mass of two prominences observed at SW limb on 20 October 2012 calculated using X-ray data with a value obtained when data in the green coronal line are used instead.



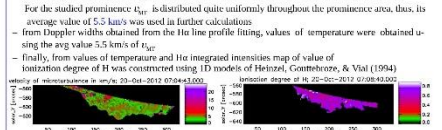
Observations in the five AIA channels used in the mass estimations. Image in the 304 Å is used for fitting the prominence area. In images in the channels 193, 211 and 335 Å a dark structure of the prominence due to absorption and coronal emissivity deficit is visible together with a cavity above the prominence due to emissivity deficit only. In the 171 Å channel some parts of the prominence are in bright due to H α emission in outer envelope of the prominence – these data are used for subtraction of EUV contribution from X-ray XRT data obtained with Al-mesh filter (see Schwartz et al. 2016).



In all three images obtained in X-rays by Hinode/XRT and also in the green coronal line by coronagraph at the Kislovodsk observatory mainly the cavity due to the emissivity deficit is visible. Although the X-ray observations were made 3 hours later than AIA, no substantial changes in prominence were seen in the AIA images during this time. The XRT data obtained with the Al-mesh filter were corrected for EUV contribution (Schwartz et al., 2016) using method described in Schwartz et al. (2015a) and AIA 171 Å image as the contribution as mainly at wavelengths around 171 Å. Observations in the green coronal line (GCL) were obtained with a coronagraph and spectrograph of dispersion of 0.1 Å/pixel in the 2nd order at the Kislovodsk observatory. Observations were made at heights 24 – 228 arcsec above the limb with step of 5 degrees in position angle (Makarov et al., 2006). The GCL data were calibrated according to tables of Neckel&Lab (1984).

Observations in the H α and Ca II 854.2 Å lines were made at 07:34 and 07:00 UT by the COMPS instrument (Kučera et al., 2010) equipped with the tunable Lyot filter made de la L. points through the line profiles with wavelet, step of 1.5 mÅ (owl) are scanned denser in the line cores). Calibration was made using table Neckel&Lab (1984). Images are not exactly co-aligned with the AIA data.

Velocity of microtubules, temperature and ionization degree of H obtained from the COMPS observations in the H α and Ca II 854.2 Å lines
 – both H α and Ca II 854.2 Å line profiles at the prominence were fitted using simple cloud model (with constant source function) and values of Doppler width were obtained
 – from Doppler widths obtained from the Ca II line profile fitting, velocity v_{H} of the microtubule was obtained (since sensitivity of v_{H} on temperature is linear because of their large atomic mass of Ca)



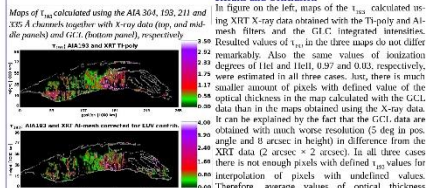
For the studied prominence v_{H} is distributed quite uniformly throughout the prominence area, thus its average value of 5.5 km/s was used in further calculations.
 – from Doppler widths obtained from the H α line profile fitting, values of temperature were obtained using the avg value 5.5 km/s of v_{H}
 – finally, from values of temperature and He I integrated intensities map of value of ionization degree of He was constructed using 1D model of Hezel, Gombosi, & Val (1994)

Detailed information about cloud-model fitting of the H α and Ca II lines and estimation of the ionization degree of H can be found in Schwartz et al. (2015a)

Values of optical thickness τ_{500} from AIA 193 and XRT X-ray/GCL data and prominence mass
 Values of optical thickness τ_{500} for wavelengths below head of the Lyman continuum of H was calculated using formula:

$$\tau_{500} = -\ln \left(\frac{I_{500}}{I_{500}^{\text{ref}}} \right)$$

 where I_{500} is ratio of EUV intensity (AIA channels 193, 211, 335 Å) to XRT X-ray/GCL intensity within the prominence area, while XRT X-ray/GCL intensities along tangential cuts through prominence are fitted to EUV lines in cavity and surrounding quiet corona. The owl asymmetry of coronal emissivity in front of and behind the prominence is estimated from comparisons of ratio of τ_{500} values obtained from the observations in two channels with the theoretical one (knowing ionization degrees, I of H and j_{λ} of He I, He II, resp., see Antez&Heinzel 2005). Values of ionization degrees, I of H and He I are estimated iteratively. Subsequently, column mass of H and He prominence plasma is derived from the τ_{500} values and total mass is obtained by integration of the column mass found over the whole prominence area. More details on the whole method can be found in Schwartz et al. (2016)



Results and Conclusion
 In figure 1, left, maps of the τ_{500} calculated using XRT X-ray data obtained with the T-poly and Al-mesh filters and the GCL, integrated intensity (rounded values of τ_{500}) in the three maps do not differ remarkably. Also the same values of ionization degrees of He I and He II, 0.97 and 0.03, respectively, are estimated in all three cases. Now, there is much smaller amount of pixels with defined value of the optical thickness in the map calculated with the GCL data than in the maps obtained using the X-ray data. It can be explained by the fact that the GCL data are obtained with much worse resolution (5 deg in position angle and 3 arcsec in height) in difference from the XRT data (2 arcsec \times 2 arcsec). In all three cases there is not enough number of pixels with defined τ_{500} values for interpolation of pixels with undefined values.
 Therefore average values of optical thickness calculated from defined pixels only were used for mass calculations. Because, the GCL data were obtained only at heights above 20 arcsec, only part of the prominence area above this height was taken into mass calculation for all three cases. Values of mass, $M_{\text{H}} = 1.5 \times 10^{24}$ g and 1.2×10^{24} g do not differ remarkably. Thus, the GCL intensities can be used instead of X-ray data in prominence mass estimations.
 Calculating more parameters is necessary for a more reliable conclusion.

REFERENCES:
 Antez, U., & Heinzel, P. 2005, A&A, 622, 714
 Hezel, P., Gombosi, P., & Val, J. C. 1994, A&A, 282, 556
 Kučera, A., Ambroz, J., Gonty, P., Kozák, M., Rybák, J. 2010, Contrib. Astr. Obs. Skalnaté Pleso, 40, 133
 Nečekal, V. J., Tlatov, A. G., Calabrese, D. K., 2006, Sol. Phys., 237, 201
 Neckel, H., Labs, D., 1984, Sol. Phys., 90, 205
 Schwartz, P., Heinzel, P., Kočik, P., Hájník, J., Krupálová, V. A. et al., 2015a, A&A 574, A62
 Schwartz, P., Hájník, S., Heinzel, P., Antez, U., Jiříben, P. R. 2015b, A&A, 587, 97

Cold plasma rotation in the tornado-like prominence of July 13, 2014: a real motion or an illusive effect?

J. Rybák, J. Ambroz, P. Gómský, J. Kavka, J. Kozák, A. Kučera, P. Schwartz, S. Tomczyk, S. Sewell, G. Capobianco, S. Fineschi, M. Temmer, V. Počl
 Astronomical Institute, SAS, Tatranská Lomnica (Slovakia), * High Altitude Observatory, NOAA, Boulder (USA), ** INFN - Astrophysical Observatory of Trieste, Pula (Trieste, Italy), *** Institute of Physics, University of Graz (Austria)

Abstract: We analyze in a case study the tornado-like prominence of July 13, 2014 which shows changing position in the SDO/AIA imaging at EUV wavelengths, using the Hinode XRT spectroscopic data acquired with the COMPS instrument (Lomnický Peck Observatory – LSO, AAS, Slovakia). The aim of the study is to address the question whether this structure is a real tornado (prominence legs plasma rotating around central axis) or we just observe illusive signatures of an apparent rotational motion, like oscillation. Our case study results indicate that as the detected Doppler shifts do not show a permanent blue/red-shift pattern along the vertical axis of the structure during the whole 45 min observing time interval, but the present variations of the Doppler shifts (a few km/s) are not in general clearly correlated with the He I integral line emission of the structure, or the Doppler shift variations do not show any regular oscillatory behaviour. These results lead to conclusion that the Doppler shifts of this particular tornado-like structure cannot be interpreted as real cold plasma rotation around the vertical axis of the structure. However the purely imaging SDO/AIA observations show clear illusive vortical motions in this tornado-like structure. We suggest that the ‘vortical illusion’ (Panusenco et al., 2014) – a combination of the counter-streaming flows in the prominence threads and possible radiative transfer effects – are causing the apparent rotational motion of this tornado-like structure.

Introduction
 Recent observations of the SDO/AIA instrument (Lemen et al., 2012) have revitalized phenomenon of solar tornado-like prominences (Ponfi, 1992). These tornado-like structures, seen as vertical prominence legs above the solar limb, are showing changing positions in the SDO/AIA imaging suggesting a rotational motion around their axis (Panusenco et al., 2014; Mghribi et al., 2016; Levens et al., 2017). Such tornado rotation around its axis was spectroscopically confirmed from helioseismic emission surrounding the structure (Jia et al., 2014; Levens et al., 2015) using the Hinode-FIB spectrograph (Kougo et al., 2007) though Young et al. (2012) pointed out that such rotation could be caused by an instrumental effect. On the other hand, the cool material ($\sim 10^4$ K) emission does not present clear signatures of rotation in two investigated cases so far (Orszós Szuez et al., 2012; Schneider et al., 2017). Panusenco et al. (2014) explained the apparent vortical motions in prominences – only observed at projection of the limb – as counterstreaming flows giving the illusion of rotation. We try to address the question, using the LSO/COMPS spectroscopic observations of a similar structure, whether it is a real tornado or we just observe illusive signatures of an apparent rotational motion.

The target tornado-like structure: SDO/AIA and LSO/COMPS data
 • July 13, 2014, south from AR 12110, above the SW limb (47°35'–63°7')
 • visible as a dark structure in all SDO/AIA UV channels (except 9.4 nm)
 • the dark structure is rotated vertically in front of the limb (Fig. 1)
 • plate-of-sky motion in several parts of the structure (Fig. 3, upper panels)
 • SDO/AIA dark structure – COMPS He I integral line emission structure, whether it is a real tornado or we just observe illusive signatures of an apparent rotational motion.

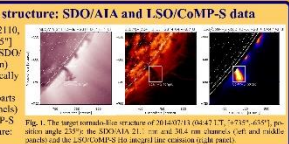


Fig. 1. The target tornado-like structure of 20140713_0447:05:22 UT. The left panels show the SDO/AIA 211, 171, and 193 Å channels (left and middle panels) and the LSO/COMPS 0.1 keV integral line emission (right panel).

LSO instrumentation & COMPS observations
Instrumentation:
 • ZEISS 500/1000 Lyot coronagraph (Leica, 1963)
 • COMPS instrument: tunable 4-stage Lyot filter with Stokes polarimeter (Kučera et al., 2011)
COMPS Observations:
 • date/time/observer: 20140713_04:47:05:22 UT, J. Kavka
 • FeV: 800°, 600°, position angle 235°
 • spectral line: He I 662.28 nm (9 points, 0.025 nm step, 98 scans)
 • filter passband width: FWHM = 0.81 nm (measured)
 • exposure time: 50 ms, scan time: 22 s
 • detector: PCO SLMC camera: 2560*2160 6.5 μm pixels
COMPS DATA REDUCTION:
 • photometric data reduction
 • Stokes parameter data only
 • 644 pixel fitting for the resulting 1.33'' pixel spatial sampling
 • sky background and the instrumental scattered light removed
 • post-fine image filter correction
 • rest line wavelength correction
 • Gaussian profile fitting to the individual He I spectral line profiles
 • the temporal (cross) smoothing of the Gaussian fit parameters
 • sub-arcsecond collimation to the SDO/AIA coordinates

The tornado-like structure zoom
 • A zoom area just around the SDO/AIA image of the tornado-like structure itself (Fig. 2)
 • the COMPS data mask: a radial overcollimating for 13'' above the solar limb
 • as manually introduced, He I integral line emission mask (9 000 Å) leading to the COMPS structure body covering the whole SDO/AIA 211 nm channel structure body (Fig. 2)
 • the masked zoom area filled with 20 adjoining 2'' wide and 52'' long pseudo-slits (parallel to the local limb) for an individual time-space analysis of the target tornado-like structure evolution
 • two pseudo-slits (P10 and P16) selected in the target structure for an illustrative display of the time-space data (Fig. 3)

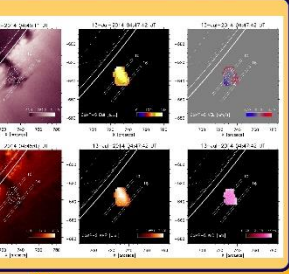


Fig. 2. Zoomed-in view of the target tornado-like structure in the background of the COMPS measurements. The SDO/AIA 211, 171, and 193 Å channels (left panels) and the LSO/COMPS 0.1 keV emission (right panel) are shown. The He I integral line emission mask (9 000 Å) leading to the COMPS structure body covering the whole SDO/AIA 211 nm channel structure body (Fig. 2) is shown. The masked zoom area filled with 20 adjoining 2'' wide and 52'' long pseudo-slits (parallel to the local limb) for an individual time-space analysis of the target tornado-like structure evolution. Two pseudo-slits (P10 and P16) selected in the target structure for an illustrative display of the time-space data (Fig. 3).

Motions in the target tornado-like structure
 • Two representative pseudo-slits (P10 and P16) selected for presentation of results in a score and in the top of the COMPS structure body (Fig. 3: left and right panels, respectively)
 • clear apparent vortical motions in the SDO/AIA intensity images lead to a typical time-space behaviour of this tornado-like structure: variable/inclined tracks in the intensity variations (Fig. 3, the top panels)
 • He I line emission locally is changing relatively to the AIA 211 and 304 nm dark structure (Fig. 3, overlays in the top panels)
 • the Doppler shifts do not show a permanent blue/red-shift pattern along the vertical axis of the structure during the whole observing time interval although there are short time intervals (~ 10 minutes) of the opposite Doppler shifts across the structure
 • in general, the Doppler shifts variations are not clearly matching the He I integral line emission or the EUV AIA intensity behaviour
 • the Doppler shift variations do not show any regular oscillatory behaviour in time

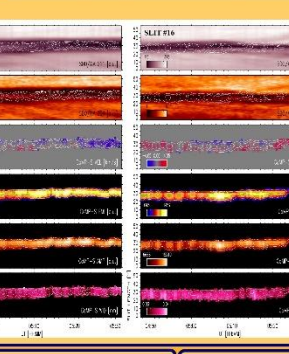


Fig. 3. The pseudo-slits P10 and P16: the time-space plots of the SDO/AIA 211 nm and 304 nm dark structure intensities (upper panels) and the LSO/COMPS He I integral line emission (middle panels) and the He I integral line emission (bottom panels) for the pseudo-slits P10 and P16. The Doppler shifts are not clearly matching the He I integral line emission. The Doppler shifts variations are not clearly matching the He I integral line emission or the EUV AIA intensity behaviour. The Doppler shift variations do not show any regular oscillatory behaviour in time.

Conclusions
 Our results lead to the conclusion that the Doppler shifts of the particular target tornado-like structure cannot be interpreted as real cold plasma rotation around the vertical axis of the structure. However the purely imaging SDO/AIA observations show clear illusive vortical motions in He I tornado-like structure. This combination of results derived from the cool plasma spectroscopy and the SDO/AIA imaging bears a resemblance to results presented already for a similar structure by Schneider et al. (2017). We suggest that the ‘vortical illusion’ (Panusenco et al., 2014) – a combination of the counter-streaming flows in the prominence threads and possible radiative transfer effects in the cold plasma blobs in the prominence (Fig. 4) – are causing the apparent rotational motion of this tornado-like structure.

Fig. 4. The filament corresponding to the target tornado-like structure (Fig. 3) in the zoomed-in view more than 1.5 days before the prominence SDO/AIA imaging and the COMPS spectroscopic observations showing the directional filament flows located mostly in the P-2 region.

REFERENCES:
 Ambroz, J., Gonty, P., Kozák, M., Rybák, J., 2010, A&A, 518, 99
 Capobianco, G., Fineschi, S., Heinzel, P., 2006, A&A, 456, 107
 Calabrese, D., Kozák, M., Gonty, P., 2006, A&A, 456, 107
 Gombosi, P., 1992, Sol. Wind, 26, 289, 60
 Hezel, P., Kočik, P., 2005, A&A, 438, 148
 Kougo, T., Saito, T., Sato, N., et al., 2007, A&A, 467, 497
 Levens, J., Tomczyk, S., Sewell, S., et al., 2017, A&A, 607, A19
 Levens, J., Schneider, B., Lomnický, S., et al., 2015, A&A, 587, 97
 Mghribi, A., Tomczyk, S., Sewell, S., et al., 2016, A&A, 593, 107
 Orszós Szuez, E., Tomczyk, S., Sewell, S., et al., 2012, A&A, 544, 107
 Panusenco, S., Tomczyk, S., Sewell, S., et al., 2014, A&A, 566, 107
 Ponfi, G., 1992, Sol. Wind, 26, 289, 60
 Schwartz, P., Gómský, P., Kozák, M., Rybák, J., 2015a, A&A, 574, A62
 Schwartz, P., Gómský, P., Kozák, M., Rybák, J., 2015b, A&A, 587, 97

Acknowledgment: This work was supported by the project VEGA 2/0004/16 of the Science Agency and by the project ITMS No.2622012002, based on the European Operational Research and development program financed from the supporting regional Development Fund.

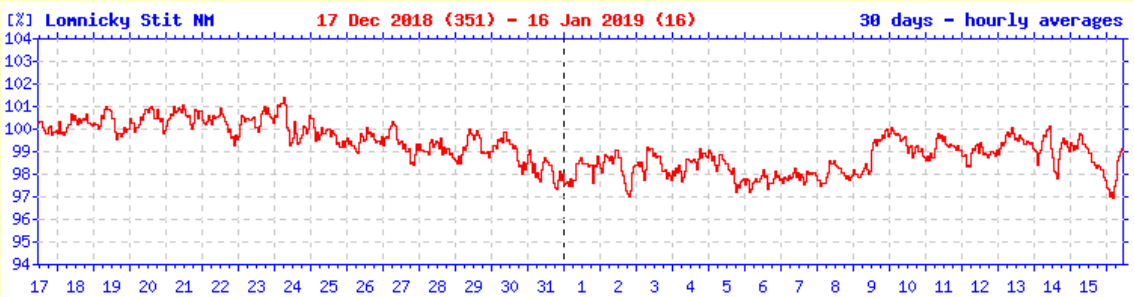
- Institute of Experimental Physics, SAS, Košice**
(Department of Space Physics)

- Energetic particles in space (solar, interplanetary, magnetospheric processes)
- Ground based observations at Lomnický štít:

1. Cosmic rays

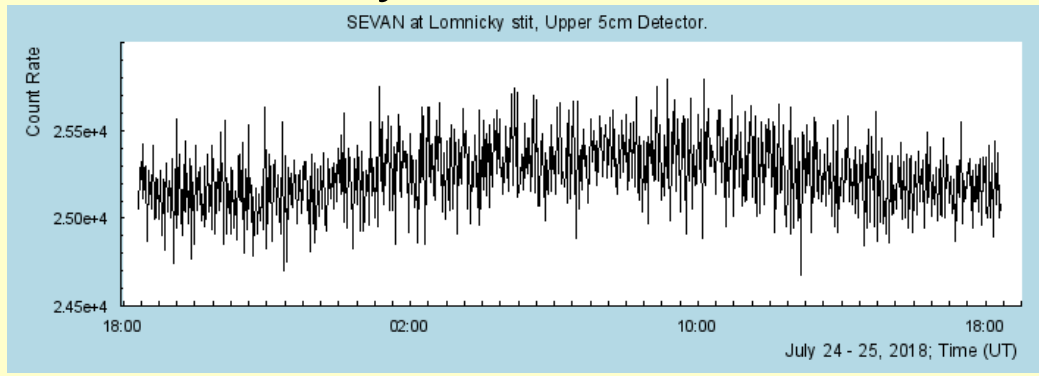
<http://neutronmonitor.ta3.sk>

and space weather:



2. Atmospheric electricity and secondary cosmic radiation:

particle detector SEVAN:

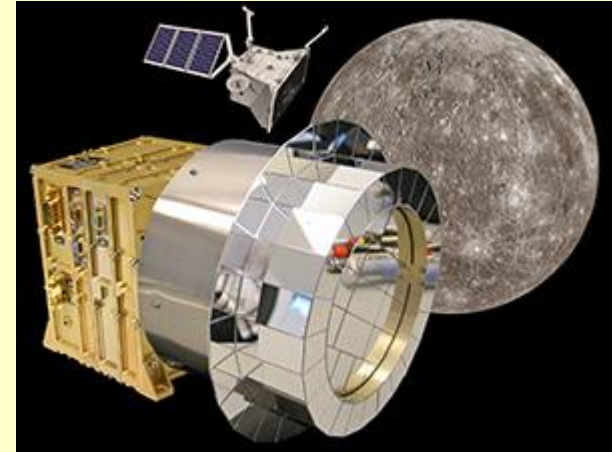


http://crd.yerphi.am/Lomnický_stit_SEVAN_Data

Space program of the IEP SAS, Košice

Mission presently in orbit: BepiColombo (ESA, 2018)

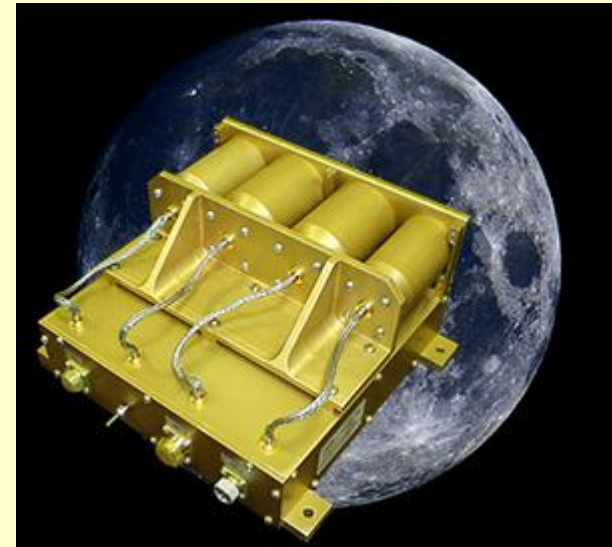
- contribution to the construction of the device **SERENA/PICAM** which will provide the mass composition, energy and angular distribution of low energy ions up to 3 keV in the environment of planet Mercury.



Mission under preparation: LUNA-GLOBE (IKI-RAN, Russia, 2020)

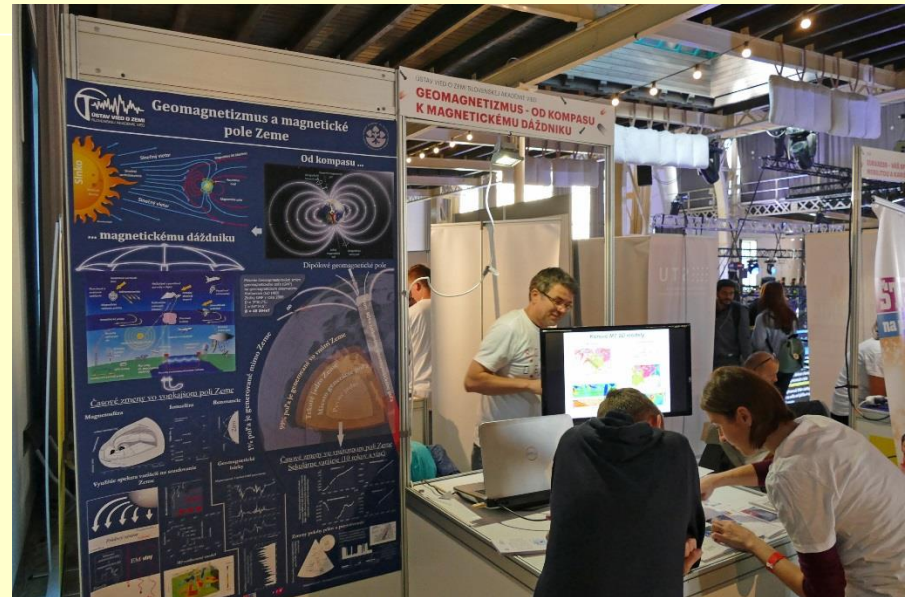
- contribution to the construction of the device **ASPECT-L** dedicated for detection of charged energetic particles temporal evolution and energy sampling on board of LUNA GLOBE orbiter.

- More at <http://space.saske.sk>

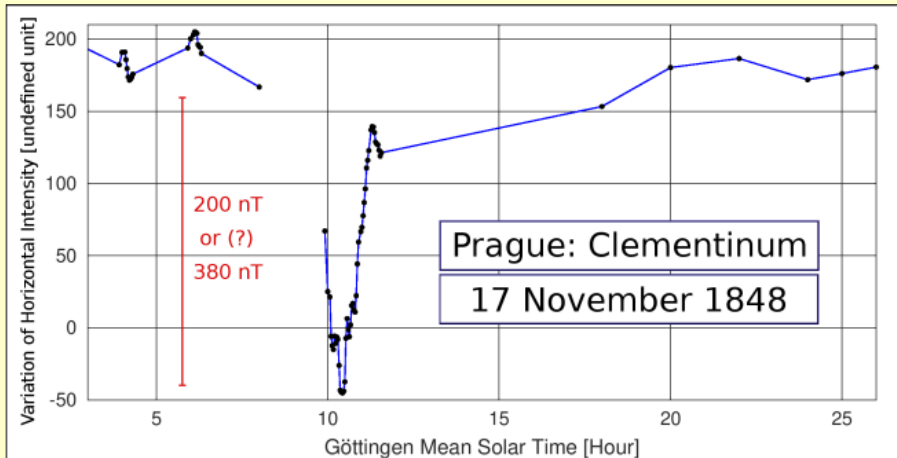


- **Earth Science Institute of SAS, Geophysical Division, Department of Geomagnetism**
- Magnetospheric physics, geomagnetic measurements in the Geomagnetic Observatory in Hurbanovo
- Mechanisms of extremely intensive geomagnetic disturbances registered in the middle latitudes

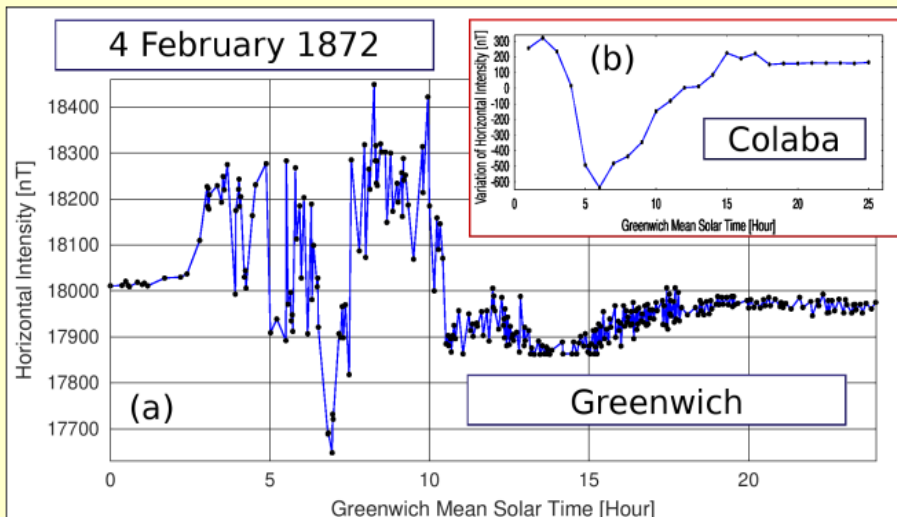
Presentation of activities related to geomagnetism, cosmical geophysics and space weather during 'European Researchers' Night, Bratislava, 28 September 2018



- Study of historical geomagnetic records and search for extreme geomagnetic activity



Two records of rapid mid-latitude magnetic storms recorded by historical magnetic observatories (years 1848 and 1872).



The profiles of the horizontal magnetic field component show that, instead of the ring current, some currents related to the auroral oval or **field aligned currents (FACs) probably played an important role in the development of these interesting geomagnetic variations.**

- **Faculty of Mathematics, Physics and Informatics,
Comenius University Bratislava**

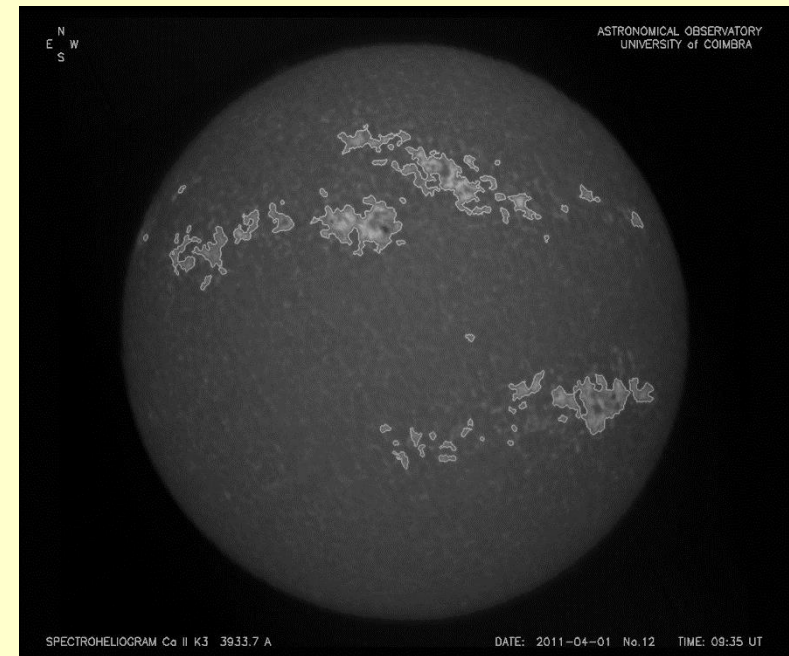
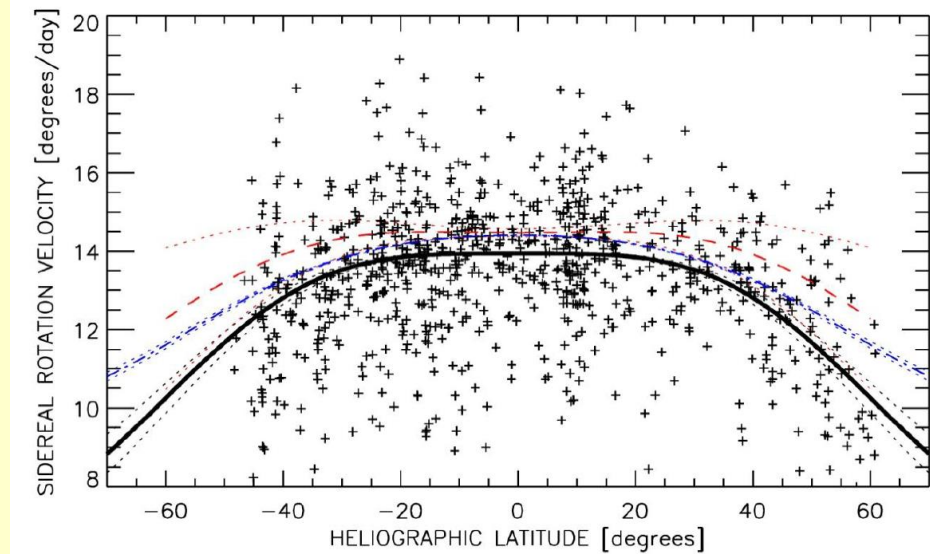
- cosmogenic nuclides (simulation of particle fluxes and cosmogenic nuclide production in the Earth's atmosphere,
- links of cosmic rays to environmental studies

**More details on space research in Slovakia
at <http://nccospar.saske.sk>**

- **Slovak Central Observatory, Hurbanovo**

- Differential rotation of the solar corona using SDO images (with UNINOVA, Lisbon, Portugal)

- Automatic detection of chromospheric plages using Calcium spectroheliograms (with OGAUC, Coimbra, Portugal)



- **National Solar Physics Meeting** organized by the SCO: 24th NSPM, 21-25 May 2018, Kežmarok.

- Ground-based observations of sunspots, prominences, flares, spectrographic observations

SOLAR ACTIVITY

(data according to observations of the Scientific Observational Dept.
of the **Slovak Central Observatory - SCO Hurbanovo**)
47°52,372' N and 18°11,368' E

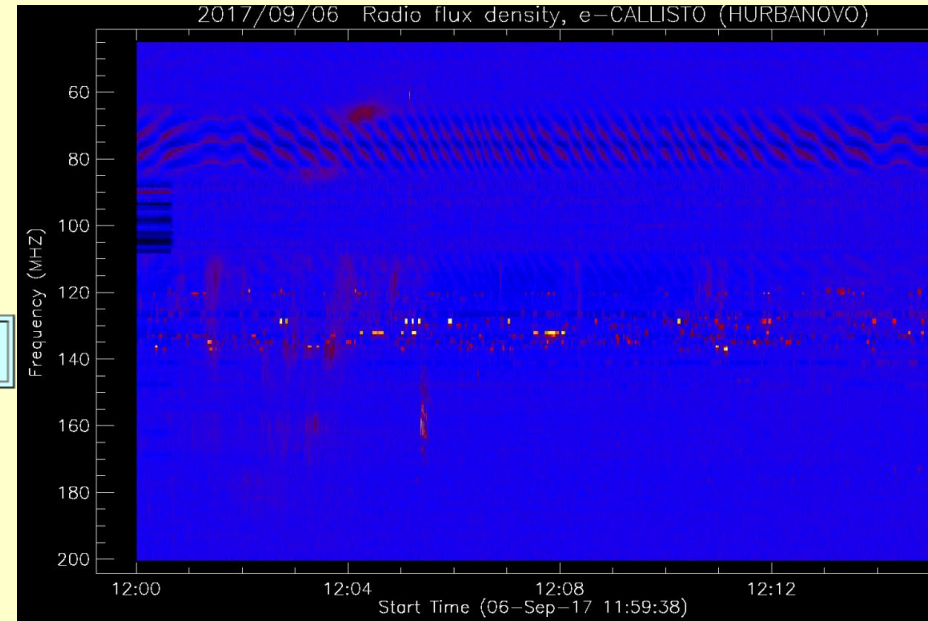
slovensky

JANUARY 2019

H-alpha Coronagraph, Heyde Dome
H-alpha filter - FWHM 0.6 nm

Coudé Refractor, Historical Building of the SCO
D/f: 150/2250 mm

CALLISTO



<http://stara.suh.sk/obs/aktivita/activity.htm>

- Modified Coronal Index: <http://www.suh.sk/online-data/modifikovany-koronalny-index>
- Modified Homogeneous Data Set of coronal intensities:
<http://www.suh.sk/online-data/modifikovany-homogenny-rad>
- 'European Researchers' Night', Hurbanovo, 28-09-2018 - presentation of activities in astrophysics, geomagnetism, and space weather

- **Daily observation of sunspots** – in many Astron. Observatories in Slovakia: data centre in Prešov
<https://astropresov.sk/na-stiahnutie/bulletin-o-pozorovani-slnka-na-slovensku/> (in Slovak)
- **SID monitoring in Slovakia** (online data):
 - Hlohovec - <http://karlovsky.info/sid/temphtml.htm>
 - Hurbanovo - http://suh.sk/index.php?option=com_content&view=article&id=392&Itemid=329
 - Partizánske -
<http://pocasiupartizanske.wz.sk/skypipepage.htm>
- **CALLISTO in Slovakia - SCO Hurbanovo**
and a radio spectrometer using a RTL-SDR receiver
in the **Hlohovec Observatory**:
<http://www.suh.sk/obs/slnsem/24css/18w.pdf>

A photograph of a sunset over the ocean. The sun is low on the horizon, creating a bright orange glow that spreads across the sky. The sky is filled with soft, wispy clouds, some of which are illuminated by the setting sun. The ocean below is dark blue with gentle waves. The overall mood is peaceful and serene.

THANK YOU!

Slovak National ISWI website: http://stara.suh.sk/id/iswi/iswi_SK-en.htm